

Article

Single-Frequency BaWO₄ Raman MOPA at 1178 nm with 100-ns Pulse Pump

Zhaojun Liu, Han Rao, Zhenhua Cong *, Feng Xue, Xibao Gao, Shang Wang, Wei Tan, Chen Guan and Xingyu Zhang

School of Information Science and Engineering, and Shandong Provincial Key Laboratory of Laser Technology and Application, Shandong University, Jinan 250100, China; zhaojunliu@sdu.edu.cn (Z.L.); raohan@mail.sdu.edu.cn (H.R.); 201511862@mail.sdu.edu.cn (F.X.); 201712302@mail.sdu.edu.cn (X.G.); 201712313@mail.sdu.edu.cn (S.W.); tanwei@sdu.edu.cn (W.T.); 201511772@mail.sdu.edu.cn (C.G.); xyz@sdu.edu.cn (X.Z.)

* Correspondence: congzhenhua@sdu.edu.cn; Tel.: +86-185-6003-6381

Received: 28 February 2019; Accepted: 27 March 2019; Published: 1 April 2019



Abstract: A single-frequency crystalline Raman master oscillator power amplifier (MOPA) at 1178 nm was demonstrated. The pump source was a homemade single-frequency 1062 nm Nd:GGG MOPA system with a pulse width of 104 ns. The BaWO₄ Raman oscillator generated seed radiation at 1178 nm with a pulse energy of 7.7 mJ. The highest amplified Raman pulse energy of 41.0 mJ was obtained with a pulse width of 44.1 ns. The linewidth was less than 500 MHz.

Keywords: crystalline Raman amplifier; single-frequency; BaWO₄ crystal

1. Introduction

During the past several decades, stimulated Raman scattering (SRS) has become an efficient method for nonlinear optical frequency conversions [1–10]. Through varieties of Raman oscillators, novel laser lines have been generated from different Raman media. In a high-power Raman laser field, R. J. Williams et al. obtained 381 W of diamond Raman laser in 2015 [5], which represented the highest power level in bulk Raman oscillators and proved the great potential for high-power applications with SRS.

Besides Raman oscillators, Raman amplifiers have also attracted much attention [11–21]. Y. Feng's group made great achievements with fiber Raman amplifiers [11–13]. In 2014, they demonstrated a 1.28 kW all-fiber Raman fiber amplifier at 1120 nm [12]. Fiber Raman amplifiers are suitable for continuous-wave (CW) lasers and low peak power pulsed lasers. While, in many applications (Light Detection and Ranging (LIDAR), range meters, and so on) [14,15], it is necessary for Raman laser pulses to possess high pulse energy, high peak power, and good spectral purity. A crystalline Raman amplifier is more suitable for these applications.

There are some reports on crystalline Raman amplifiers [16–21]. But spectral purity was not concerned [16–20]. These Raman amplifiers all operated under multi-longitudinal-mode state. In 2015, we demonstrated a single-frequency crystalline Raman amplifier [21]. The output pulse energy at 1178 nm was 26.7 mJ with a pulse width of 2.9 ns. Raman amplification could only occur during a certain intensity range. The short pulse width limited the power scaling. Under the same beam size, shorter pulse width led to higher intensity. If the intensity was high enough, stimulated Raman generation would occur instead of Raman amplification.

In this paper, we realized a 100-ns pulse pumped single-frequency BaWO₄ Raman MOPA system. The pump source was a homemade single-frequency 1062 nm Nd:GGG MOPA system with a pulse width of 104 ns. With this long pulse duration, higher pulse energy was expected at the same level

of pumping intensity. From an extra-cavity BaWO₄ Raman oscillator, 7.7 mJ of 1178 nm laser was obtained. Through two stages of BaWO₄ Raman amplification, Raman pulse energy of 41 mJ was obtained with a pulse width of 44.1 ns. The linewidth was determined to be less than 500 MHz.

2. Experimental Setup

A schematic diagram of the single-frequency BaWO₄ Raman MOPA is illustrated in Figure 1. We have previously reported an LD pumped single-longitudinal-mode (SLM) passively Q-switched Nd:GGG laser [22]. It was used as the master laser for the 1062 nm MOPA. We can obtain different output pulse width and energy by replacing the saturable absorber with different initial transmission. In this work we chose a saturable absorber with an initial transmission of 83%. Pulse energy of 160 μJ and pulse width of 84 ns were obtained. The amplification stages were flash-lamp-pumped Nd:GGG modules. From this MOPA system, the highest output energy was 460 mJ, with a pulse width of 105 ns, and a repetition rate of 5 Hz. The diameter of the 1062 nm laser beam was 3.5 mm.

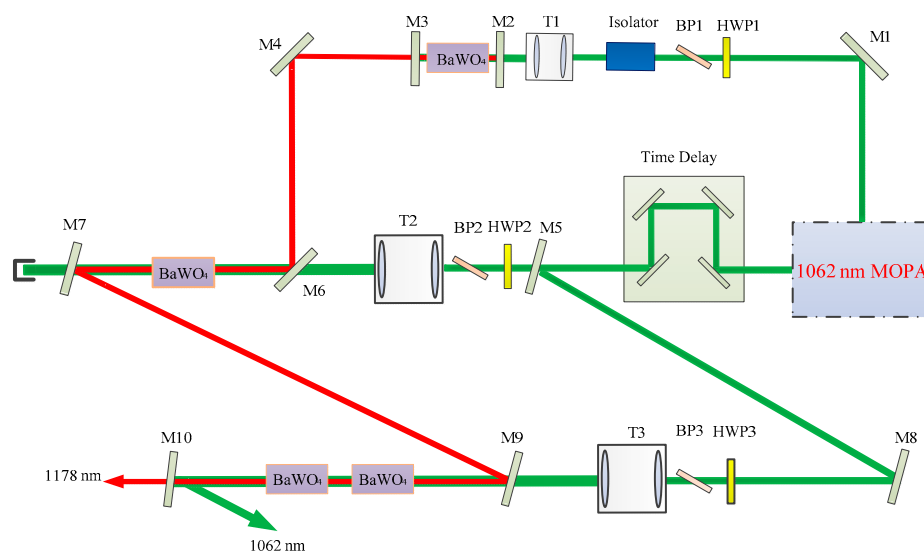


Figure 1. Schematic of single-frequency BaWO₄ Raman master oscillator power amplifier.

1062-nm laser pulse with energy of 60 mJ was directed into an extra-cavity Raman oscillator between M2 and M3. All the mirror parameters are shown in Table 1. The output coupler (M3) was coated for high reflection at 1062 nm to form a two-passing pumping scheme. A Faraday isolator was used to avoid the feedback pump beam. The Raman gain medium was an a-cut BaWO₄ crystal with a size of 7 mm × 7 mm × 87.8 mm and anti-reflection (AR) coatings at 1062 nm and 1178 nm ($R < 0.2\%$) on both facets.

1062-nm laser pulse with energy of 400 mJ was used as the pumping source for Raman power amplifiers. Through M5, 100 mJ and 300 mJ pumping pulse energies were incident into the first and second stage amplifiers, respectively. Another three-cut BaWO₄ crystals with size of 7 mm × 7 mm × 87.8 mm were employed in the Raman power amplifiers. One was placed in the first stage and the other two was placed in the second stage. All the three BaWO₄ crystals were uncoated.

Three half-wave plates (HWP1, HWP2, and HWP3) and Brewster polarizers (BP1, BP2, and BP3) were used to adjust the pump energy and polarization direction. The pump beam size was controlled by three telescopes (T1, T2, and T3). A time delay line was used to adjust the optical path of the pump laser to realize good temporal overlap of the pump and the Raman signal pulses.

Laser pulse energy was measured by a pyroelectric energy sensor (J-50MB-LE) with a laser energy meter (Lab Max-Top). Temporal characteristics of laser pulses were monitored by a fast detector (DET10N/M, Thorlabs) and an oscilloscope (WaveRunner 606Zi, Teledyne Lecroy).

Table 1. Mirror parameters.

No.	Radius of Curvature	Coatings	Incident Angle
M1	∞ - ∞	R > 99%@1062 nm	45°
M2	∞ - ∞	T > 98%@1062 nm & R > 99.5%@1178 nm	0°
M3	∞ -1000 mm (concave)	R > 99.8%@1062 nm & R = 75%@1178 nm	0°
M4	∞ - ∞	R > 99%@1178 nm	45°
M5	∞ - ∞	R = 75%@1062 nm	20°
M6	∞ - ∞	T > 98%@1062 nm & R > 99%@1178 nm	45°
M7&M9	∞ - ∞	T > 99%@1062 nm & R > 99%@1178 nm	15°
M8	∞ - ∞	R > 99%@1062 nm	20°
M10	∞ - ∞	R > 99.8%@1062 nm & T > 99%@1178 nm	0°

3. Results and Discussion

The output characteristics of the 1178 nm Raman oscillator were investigated firstly. The output Raman pulse energy and pulse width with respect to pump pulse energy are shown in Figure 2. The pump beam size was controlled to be 2.5 mm through T1. The beam profile was monitored by a CCD camera (BeamOn HR). As shown in Figure 2, the threshold of Raman oscillator was 28 mJ. The maximum output energy of 7.7 mJ was obtained at pump pulse energy of 58 mJ. The pulse width was 49.0 ns.

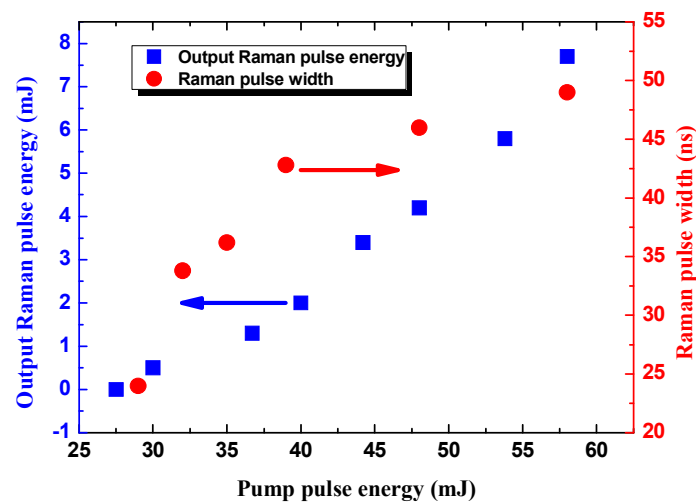


Figure 2. Output Raman pulse energy and pulse width versus the pump pulse energy.

The optical spectrum was monitored through a high-resolution spectrum analyzer (Yokogawa AQ6370D). The center wavelength was measured to be 1178.3 nm. At the highest pump level, no higher order Stokes waves were observed. By using Fabry–Perot (F–P) interferometry method [23], we confirmed that the Raman laser operated with single longitudinal mode.

Raman pulse with energy of 7.7 mJ was injected to the first-stage amplifier. The beam diameters of the Raman signal and pump laser were 2.8 mm and 3.0 mm, respectively. Spatial overlapping of signal and pump laser beams was monitored on the CCD. By adjusting the time delay line, temporal overlapping of signal and pump laser was also finished. The oscilloscope traces of the pump and signal pulses for the first-stage amplifier are presented in Figure 3a. The two pulses were well synchronized.

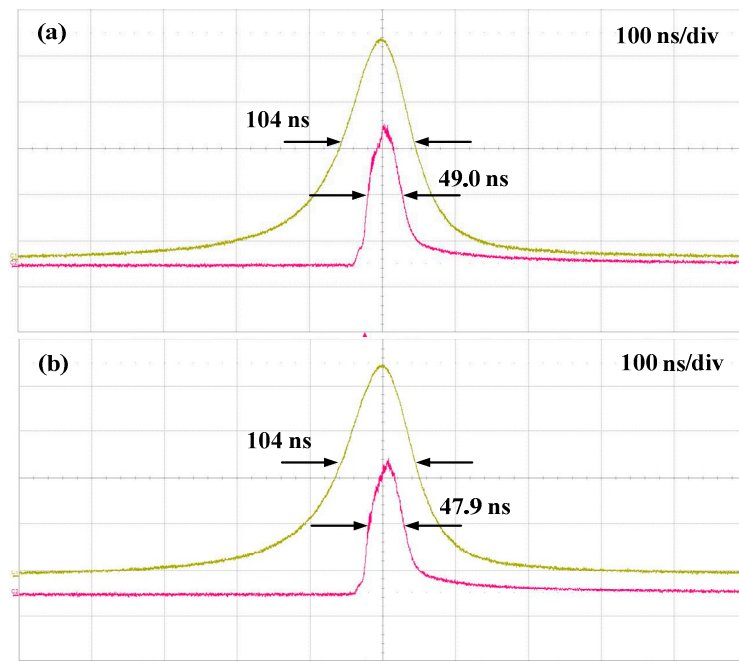


Figure 3. Oscilloscope traces of pump (**upper**) and Raman (**lower**) laser pulses: (a) first-stage amplifier and (b) second-stage amplifier.

Figure 4a shows the output Raman pulse energy of the first-stage amplifier as a function of the pump pulse energy. The highest output pulse energy of 12.0 mJ was obtained at pump pulse energy of 92.0 mJ. The pulse duration was 47.9 ns, as shown in Figure 3b. In the beginning, the BaWO₄ crystal was coated for antireflection at 1062 nm and 1178 nm. The coating was damaged when the pump pulse energy was increased to its maximum. The damage threshold of coating was calculated as ~ 1.42 J/cm². To avoid damages, we chose uncoated BaWO₄ crystals during the whole work.

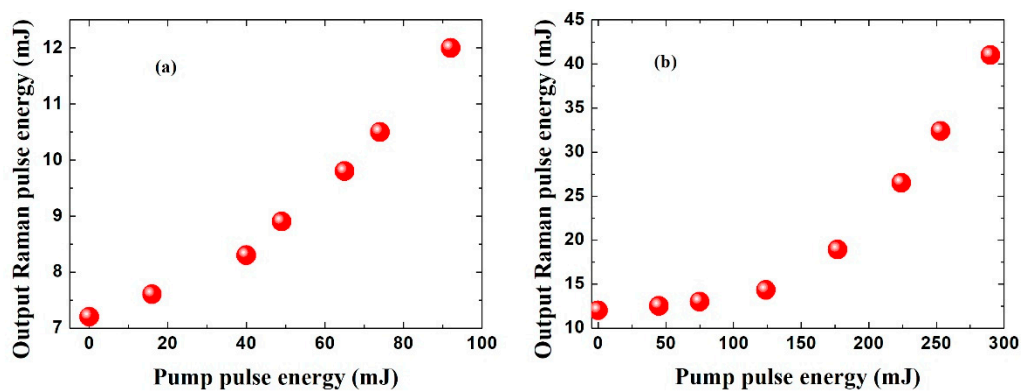


Figure 4. Output Raman pulse energy versus pump pulse energy of the Raman power amplifiers: (a) first-stage and (b) second-stage.

The amplified Raman pulse from the first-stage was used as the signal for the second-stage amplifier. The signal pulse energy was fixed at 12.0 mJ. The pump and signal pulses were also overlapped in time, as shown in Figure 3b. The beam diameters of the signal and pump laser beams were 3.2 mm and 3.5 mm, respectively. The amplified Raman pulse energy of the second-stage with respect to the pump pulse energy is shown in Figure 4b. At a pump pulse energy of 290 mJ, the highest output Raman pulse energy was 41.0 mJ, corresponding to an extraction ratio of 10%. The Raman laser pulse width was 44.1 ns.

It was crucial to control the pump power density. If it was too high, stimulated Raman generation would occur instead of Raman amplification. When blocking the Raman oscillator, we did not observe any Raman laser output at the end of the amplifiers. This proved that we realized Raman amplifications in our experiments.

In the first stage, the amplification ratio was low. The main reason was low Raman gain induced by the low pump intensity. At the highest pump level of 92.0 mJ, the peak power density was only 13 MW/cm². Due to the lack of proper beam reducer, we were not able to realize higher power density in the first stage. In the second stage, the highest peak power density was 30.1 MW/cm² and the Raman crystal length was doubled. As a result, we obtained a higher extraction ratio of 10%. This extraction ratio was comparable with our previous result [21].

By using a F–P interferometer with a free spectral range (FSR) of 5.4 GHz, we measured the linewidth of amplified Raman radiation. Both faces of F–P had high reflection (HR) coatings ($R > 95\%$) at 1178 nm. The interference pattern of the Raman laser was received with a CCD, as shown in Figure 5. It was found that the laser operated with single longitudinal mode. According to the method used in our previous work [21], the linewidth of the 1178 nm Raman laser was calculated to be less than 500 MHz.

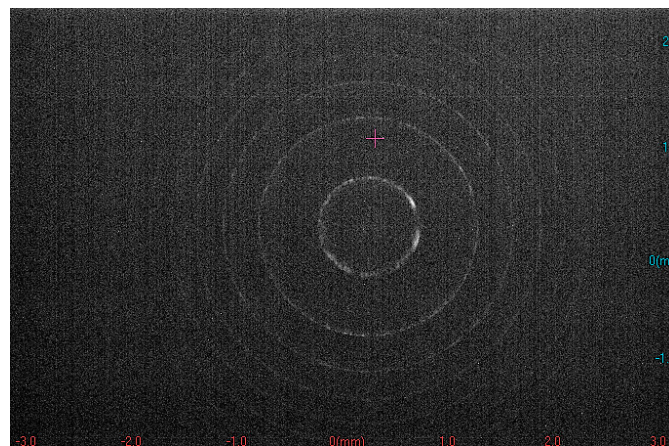


Figure 5. Typical interference pattern of the single-frequency 1178 nm Raman laser.

In our former work [21], a laser beam with much shorter pulse duration of only 7 ns was used. While in this experiment, a 1062 nm laser beam with long pulse duration of 104 ns was employed as the pump source. Despite this, we still realized a comparable extraction ratio with much lower peak power here. The main reason limiting power scaling here was the 1062 nm laser pulse energy. The Nd:GGG crystal rods at hand were not high-quality. The scattering centers and optical inhomogeneity of the Nd:GGG crystals limited the power scaling of 1062 nm laser. With a better 1062 nm pulsed laser, we would obtain higher amplified Raman pulse energy. We can still claim that our design in this paper was promising for higher Raman amplifier power.

4. Conclusions

We have demonstrated a high energy single-frequency crystalline Raman MOPA at 1178 nm with a hundred-nanosecond pulsed laser pump. The overall system was introduced in this paper, including the single-frequency Nd:GGG MOPA, single-frequency BaWO₄ Raman oscillator, and power amplifiers. The Nd:GGG MOPA system provided 460 mJ pulse energy at 1062 nm with a pulse duration of 104 ns. The output energy of Raman oscillator was 7.7 mJ. With two stages of Raman power amplifications, the output pulse energy at 1178 nm was amplified to 41.0 mJ, and the pulse width was 44.1 ns. The Raman MOPA operated with single longitudinal mode. The linewidth was calculated to be less than 500 MHz.

Author Contributions: Conceptualization, Z.C. and Z.L.; methodology, H.R., F.X. and Z.L.; validation, X.G. and S.W.; investigation, W.T. and C.G.; writing—original draft preparation, H.R. and Z.L.; writing—review and editing, Z.C. and X.Z.

Funding: This work is supported by the National Natural Science Foundation of China (118041292), China Postdoctoral Science Foundation (2018M642651), the Joint Foundation from Ministry of Education (6141A02022413, 6141A02022421), the Young Scholars Program of Shandong University (2016WLJH13), and the Fundamental Research Funds of Shandong University (2018JCG02, 2017JC023).

Conflicts of Interest: The authors declare no conflict of interest.

References

1. Zverev, P.G.; Basiev, T.T.; Sobol, A.A.; Skorniyakov, V.V.; Ivleva, L.I.; Polozkov, N.M.; Osiko, V.V. Stimulated Raman scattering in alkaline-earth tungstate crystals. *Quantum Electron.* **2000**, *30*, 55–59. [[CrossRef](#)]
2. Rong, H.; Jones, R.; Liu, A.; Cohen, O.; Hak, D.; Fang, A.; Pannicia, M. A continuous-wave Raman silicon laser. *Nature* **2005**, *433*, 725–728. [[CrossRef](#)]
3. Piper, J.A.; Pask, H.M. Crystalline Raman lasers. *IEEE J. Sel. Top. Quantum Electron.* **2007**, *13*, 692–704. [[CrossRef](#)]
4. Liu, Z.J.; Wang, Q.P.; Zhang, X.Y.; Zhang, S.S.; Chang, J.; Fan, S.Z.; Sun, W.J.; Jin, G.F.; Tao, X.T.; Sun, Y.X.; et al. Self-frequency-doubled KTiOAsO₄ Raman laser emitting at 573 nm. *Opt. Lett.* **2009**, *34*, 2183–2185. [[CrossRef](#)]
5. Williams, R.J.; Nold, J.; Strecker, M.; Kitzler, O.; McKay, A.; Schreiber, T.; Mildren, R.P. Efficient Raman frequency conversion of high-power fiber lasers in diamond. *Laser Photonics Rev.* **2015**, *9*, 405–411. [[CrossRef](#)]
6. Jiang, W.; Li, Z.; Zhu, S.; Yin, H.; Chen, Z.; Zhang, G.; Chen, W. YVO₄ Raman laser pumped by a passively Q-switched Yb:YAG laser. *Opt. Express* **2017**, *25*, 14033–14042. [[CrossRef](#)] [[PubMed](#)]
7. Guo, J.; Zhu, H.Y.; Chen, S.M.; Duan, Y.M.; Xu, X.R.; Xu, C.W.; Tang, D.Y. Yellow, lime and green emission selectable by BBO angle tuning in Q-switched Nd:YVO₄ self-Raman laser. *Laser Phys. Lett.* **2018**, *15*, 075803. [[CrossRef](#)]
8. Duan, Y.M.; Zhang, J.; Zhu, H.Y.; Zhang, Y.C.; Xu, C.W.; Wang, H.Y.; Fan, D.Y. Compact passively Q-switched RbTiOPO₄ cascaded Raman operation. *Opt. Lett.* **2018**, *43*, 4550–4553. [[CrossRef](#)]
9. Frank, M.; Smetanin, S.N.; Jelínek, M.; Vyhlídal, D.; Ivleva, L.I.; Zverev, P.G.; Kubeček, V. Highly efficient picosecond all-solid-state Raman laser at 1179 and 1227 nm on single and combined Raman lines in a BaWO₄ crystal. *Opt. Lett.* **2018**, *43*, 2527–2530. [[CrossRef](#)]
10. Chen, Y.F.; Pan, Y.Y.; Liu, Y.C.; Cheng, H.P.; Tsou, C.H.; Liang, H.C. Efficient high-power continuous-wave lasers at green-lime-yellow wavelengths by using a Nd:YVO₄ self-Raman crystal. *Opt. Express* **2019**, *27*, 2029–2035. [[CrossRef](#)]
11. Feng, Y.; Taylor, L.R.; Calia, D.B. 25 W Raman-fiber-amplifier-based 589 nm laser for laser guide star. *Opt. Express* **2009**, *17*, 19021–19026. [[CrossRef](#)]
12. Zhang, L.; Liu, C.; Jiang, H.; Qi, Y.; He, B.; Zhou, J.; Gu, X.; Feng, Y. Kilowatt ytterbium-Raman fiber laser. *Opt. Express* **2014**, *22*, 18483–18489. [[CrossRef](#)]
13. Zhang, L.; Jiang, H.; Cui, S.Z.; Hu, J.; Feng, Y. Versatile Raman fiber laser for sodium laser guide star. *Laser Photonics Rev.* **2014**, *8*, 889–895. [[CrossRef](#)]
14. Oliver, L.; Han, J.R.; Haro, F.; Hans, J.E. Barium nitrate Raman laser at 1.599 μm for CO₂ detection. *Proc. SPIE* **2012**, *8677*, 86771B1-7. [[CrossRef](#)]
15. Grady, J.K.; Bruce, W.B.; Mulugeta, P.; Jeffrey, Y.B.; Farzin, A.; Jirong, Y.; Richard, E.D.; Syed, I.; Stephanie, V.; Michael, J.K.; et al. Coherent differential absorption lidar measurements of CO₂. *Appl. Opt.* **2004**, *43*, 5092–5099. [[CrossRef](#)]
16. Raghunathan, V.; Borlaug, D.; Rice, R.R.; Jalali, B. Demonstration of a mid-infrared silicon Raman amplifier. *Opt. Express* **2007**, *15*, 14355–14362. [[CrossRef](#)] [[PubMed](#)]
17. Lisinetskii, V.A.; Orlovich, V.A.; Rhee, H.; Wang, X.; Eichler, H.J. Efficient Raman amplification of low divergent radiation in barium nitrate crystal. *Appl. Phys. B* **2008**, *91*, 299–303. [[CrossRef](#)]
18. Yakovlev, V.V.; Petrov, G.I.; Zhang, H.F.; Noojin, G.D.; Denton, M.L.; Thomas, R.J.; Scully, M.O. Stimulated Raman scattering: Old physics, new applications. *J. Mod. Opt.* **2009**, *56*, 1970–1973. [[CrossRef](#)] [[PubMed](#)]
19. Kulagin, O.V.; Gorbunov, I.A.; Sergeev, A.M.; Valley, M. Picosecond Raman compression laser at 1530 nm with aberration compensation. *Opt. Lett.* **2013**, *38*, 3237–3240. [[CrossRef](#)] [[PubMed](#)]

20. Wang, C.; Cong, Z.H.; Liu, Z.J.; Zhang, X.Y.; Wang, Q.P.; Wei, W.; Li, L.; Zhang, Y.G.; Wang, W.T.; Wu, Z.G.; et al. Theoretical and experimental investigation of an efficient pulsed barium tungstate Raman amplifier at 1180 nm. *Opt. Commun.* **2014**, *313*, 80–84. [[CrossRef](#)]
21. Men, S.J.; Liu, Z.J.; Cong, Z.H.; Liu, Y.; Xia, J.B.; Zhang, S.S.; Cheng, W.Y.; Li, Y.F.; Tu, C.Y.; Zhang, X.Y. Single-frequency CaWO₄ Raman amplifier at 1178 nm. *Opt. Lett.* **2015**, *40*, 530–533. [[CrossRef](#)] [[PubMed](#)]
22. Xue, F.; Zhang, S.S.; Cong, Z.H.; Huang, Q.J.; Guan, C.; Wu, Q.W.; Chen, H.; Bai, F.; Liu, Z.J. Diode-end-pumped single-longitudinal-mode passively Q-switched Nd:GGG laser. *Laser Phys. Lett.* **2018**, *15*, 035001. [[CrossRef](#)]
23. Heard, H.G. *Laser Parameter Measurements Handbook*, 1st ed.; John Wiley & Sons: Hoboken, NJ, USA, 1968; ISBN 9780471366652.



© 2019 by the authors. Licensee MDPI, Basel, Switzerland. This article is an open access article distributed under the terms and conditions of the Creative Commons Attribution (CC BY) license (<http://creativecommons.org/licenses/by/4.0/>).